24GHz Radar Antenna on Eco-Friendly Substrate

M. E. de Cos Gómez[1], A. Florez Berdasco[1], H. Fernández Álvarez[2], F. Las-Heras Andrés[1]
[1] TSC, Electrical Engineering Department. Universidad de Oviedo. Gijón, Spain, medecos@uniovi.es
[2] EME, Antenna Systems and Signatures Engineering SP, Airbus Defense and Space, Getafe, Spain

***Abstract*— A compact and low-cost wearable grid array antenna (GAA) for 24GHz radar applications is proposed. It is designed on eco-friendly Polypropylene (PP) substrate with aluminum claddings. The overall size of the antenna is 60 x 60 x 0.52 mm3. Prototypes of the antenna are fabricated and tested, achieving results that meet typical requirements for collision avoidance applications, as the envisioned one in aid of visually impaired people. The presented antenna overcomes the state of the art on 24GHz wearable radar antennas according to a comparison based on a literature survey**

***Index Terms*— mm-wave antenna, grid array antenna, radar antenna, eco-friendly, wearable antenna.**

I. INTRODUCTION

The 24GHz ISM frequency band is allocated for radar applications such as vehicle guidance, automotive speedometers, collision warning and obstacle detection, due to the suitability of mm-wave frequencies for high resolution detection in foggy, smoky and dusty environments. All of these applications require compact, high gain and narrow beam antennas [1]. The antenna has a great impact on the radar system performance. A trade off solution between range and coverage area has to be adopted

The grid array antennas (GAAs) were introduced by Kraus [2] as travelling-wave (non-resonant) antennas with the main lobe of radiation in a backward angle-fire direction. The GAA allows achieving a high radiating element density while minimizing the number of feeding lines external to the antenna structure. Conti et al. [3] implemented them in microstrip technology as a standing-wave (resonant) antennas with the main radiation beam in the broadside direction, showing additional benefits in terms of high gain, cross polarization control and broader bandwidth over conventional patch type radiators. The works of Nakano et al. [4]-[5] also contributed to the development of GAAs. Zhang proposed using GAAs as Doppler sensors for mm-wave radar applications [6], being followed by other contribution to that aim [7]. Recent works have explored the use of optimized GAAs at lower frequencies for WIFI applications [8]. The advantages of GAAs make them suitable for the intended application of collision avoidance in the 24GHz ISM frequency band. The use of GAAs in mm-wave has hardly been explored and they have not yet been implemented on flexible, ecological and low-cost materials, with the challenges that this entails.

Awareness of the environmental impact of human activity and the scarcity of resources, as well as their potential consequences, lead to an increasingly firm step towards circular economies and green technologies. In electronics, this means, among other solutions, looking for new eco-friendly materials [9]-[12] and manufacturing technologies with a reduced ecological footprint. Recently some works have proposed mm-wave antennas on eco-friendly substrates [13]-[14], but does not apply to the metallic parts and not all them are suitable for wearable applications, due to moisture sensitivity and very limited radiation efficiency [13].

Technological limitations often impact fabrication accuracy of mm-wave antennas, even using commercial substrates, and that makes the adoption of those materials not conventionally used to that aim more challenging and the analysis on how such limitations lead to impairments on the performance much more interesting.

In this work a wearable GAA antenna, for collision avoidance at 24GHz, based on both eco-friendly substrate (Polypropylene, PP) and conductor (aluminum) is presented. First, the electromagnetic characterization of the PP at 24GHz is explained. Then the design of the antenna on both RO3003 and PP eco-friendly substrate is presented. The fabrication of prototypes is shown next, along with a detailed description of the measurement results, followed by an analysis of their matching with the simulation ones. Next, comparison with the state of the art on 24GHz radar antennas is shown. At the end, some conclusions are stated.

II. DIELECTRIC SUBSTRATES FOR THE ANTENNA

Two dielectrics are considered as antenna substrates:

A. Rogers' RO3003

It consists of ceramic-filled PTFE (Teflon) composites, with relative dielectric permittivity, ε_r=3.0, very stable with T^a and very low loss tangent, tanδ=0.0013 [15]. It is widely used in electronics. It exhibits certain degree of conformability and softness, so that it could be used for wearable antennas. It complies with Hazardous Substances (RoHS) regulation but it is not eco-friendly for being PTFE based. In this work is used as reference to compare the performance of the eco-friendly material for identical aim.

B. Polypropylene (PP)

The polypropylene (PP) is extensively used in automotive and medical applications and in food packaging due to its flexibility, lightness, resistance to fatigue and environmental benefits. It is a thermoplastic polymer that can

be recycled multiple times and it does not release as many toxins and CO_2 as other plastics (PVC, PET and PS), being much cheaper than extensively used substrates. Pioneer work on using PP as antenna substrate at low microwave frequencies [10] was successfully followed by other authors [11]-[12]. Recently, its use at mm-wave frequencies has been explored for a patch-type array [14]. However, there are still many pending challenges concerning the fabrication of antennas with more complex geometries and the reduction of mismatches between simulation and measurement results, due to impairments related to substrate characterization, manufacturing tolerances, connectorization and measurement procedure.

C. *Electromagnetic characterization of the PP at 24GHz*

Aiming at determining the relative dielectric permittivity (ε_r) and the loss tangent ($\tan\delta$) of PP at 24GHz, two characterization methods are combined. First, several measurements of a higher order mode, close to 24GHz, of a 10 GHz resonant cavity (Agilent Technologies 85072A 10 GHz split-cylinder resonator) are taken for a sample of h=0.52 mm thickness. Statistical treatment of the retrieved data yielded ε_r = 2.42 and $\tan\delta$ = 0.002, that are taken as starting point in simulation for the second method based on a microstrip line and an open-circuit resonant stub (T-resonator) at the target frequency [16]. Then, such microstrip line and T-resonator are fabricated, which helps to account, to some extent, for fabrication tolerances concerning microstrip technology, which are not considered in the former method and are crucial to get agreement between simulation and measurement results. Those ε_r and $\tan\delta$ values, retrieved in electromagnetic simulation, that match the resonance frequency position and the insertion losses obtained in measurement, are the characterization ones. ε_r=2.2 and $\tan\delta$=0.002 were obtained.

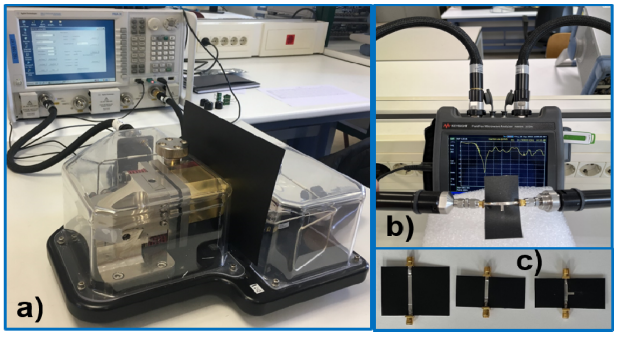

Fig. 1. Set-up for electromagnetic characterization of PP: a) Split-cylinder resonator, b) VNA and c) microstrip lines and T-resonator samples.

III. Design of the GAA antenna

The GAA (see Fig. 2) comprises 32 equally sized rectangular loops of conductors (the radiating grid) on the top surface of a dielectric substrate backed by a metallic ground plane. The number of loops controls directivity and functional bandwidth. Increasing it raises directivity but decreases functional bandwidth. The long side of each loop acts as transmission line, while the short side acts mainly as radiator, which yields 41 radiating elements in total. The resonance of the GAA requires the length of the long sides to be approximately $l=\lambda_g$ and the length of the short sides $W=\lambda_g/2$, where λ_g is the guided wavelength at the center frequency of operation [3]. Therefore, the long sides support full wavelength current (out of phase) while the current on each short side is in phase, which leads to maximum radiation broadside to the array. The widths of the long and short sides of the grid (W_l and W_s) are chosen to improve the signal propagation and to achieve the desired amplitude taper on the array. Specifically, W_l controls the losses in the transmission line and the radiation of cross-polar components. It is chosen so that W_l /h<1 for Z< 200Ω. W_s controls the radiation coefficients of the array and thus the width of the aperture and the side lobes level (SLL). The resulting optimized dimensions, using FEM based commercial 3D electromagnetic simulation software, on both RO3003 and PP dielectrics, are indicated in TABLE I.

To feed the radiating grid a coaxial probe with Teflon filling, 0.38mm probe diameter, 0.5 mm inner diameter and 0.2 mm outer diameter is drilled through the ground and the substrate. The outer conductor is connected to the ground plane, whereas the inner one is connected to the grid near its geometrical center. At the four corners of the substrate there are four holes each of 2mm diameter, to fix and flatten the antenna for measurement purposes.

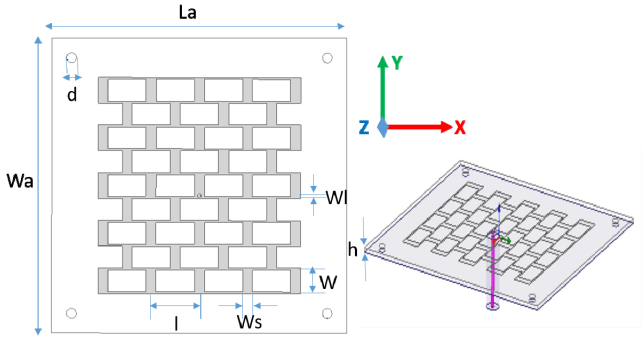

Fig. 2. Top and side view of the geometry of the grid antenna with detailed parameterized dimensions along with the feeding placement.

TABLE I. Dimensions of the optimized Array antenna design

Dielectric	Dimensions (mm)						
	L_a	W_a	h	l	W_s	W	W_l
RO3003	60	60	0.762	8.8	2.5	4.8	0.5
PP	60	60	0.52	9.8	2	5.25	0.4

A. *Impedance matching of the grid array antenna*

The designed antennas on both RO3003 and PP exhibit very good impedance matching in the target 24.05GHz – 24.25GHz band (see TABLE II.). The GAA on RO3003 is thicker although with higher ε_r. Nonetheless a tradeoff solution between bandwidth and directivity applies to GAAs.

TABLE II. FREQUENCY BAND AND BANDWIDTH OF THE ANTENNA IN SIMULATION

Dielectric	Frequency band			
	Freq (GHz)		*Bandwidth*	
	f_{LOW}	f_{UP}	*Total (MHz)*	*(%)*
RO3003	21.43	24.67	3240	14
PP	23.43	24.39	960	4

B. *Radiation Characteristics of the grid array antenna*

TABLE III. indicates the radiation characteristics of the GAA in simulation, in terms of: peak realized gain (G), peak directivity (D), radiation efficiency (η) and front to back ration (FTBR), for the center and ends frequencies of the target band. It is remarkable that, in addition to reaching high levels of G (>16dBi) and D (>17dB), which make the GAA suitable as radar sensor, optimal levels of radiation efficiency (>90%) and FTBR (>25 dB) are achieved, which are crucial for wearable applications. And furthermore, PP outperforms RO3003 in terms of G, for similar η and FTBR.

Broadside pencil-beam radiation patterns with low side lobe level (SLL) and weak cross-polarization are achieved for both RO3003 and PP. The co-polarized pattern in the E-plane (Phi=90°) is asymmetric (see Fig. 3), due to the unbalanced feeding. The resulting Side-lobe level (SLL) and Half-power beam width (HPBW), from the pattern cuts for Phi=0º and Phi=90º at the center frequency of the band (24.15GHz) shown in Fig. 3, are indicated in TABLE III. and are suitable for the envisioned application in collision avoidance radar, on both RO3003 and PP dielectrics. The 3dB gain-drop bandwidth is almost identical for both materials, being the PP thinner, lighter and more flexible.

TABLE III. RADIATION PROPERTIES RESULTS IN SIMULATION

Dielectric	**Freq (GHz)**	**G (dBi)**	**D (dB)**	**η (%)**	**FTBR (dB)**
RO3003	24.05	18	18.1	98	27.9
	24.15	17.6	17.8	96	27.7
	24.25	16.9	17.2	95	27.7
PP	24.05	21	21.1	98	25.6
	24.15	20.8	20.9	98	25.7
	24.25	20.4	20.6	96	25.8
\ @ 24.15 GHz	**Radiation Bandwidth (GHz)**	**SLL (dB) φ=0º**	**HPBW (º) φ=0º**	**SLL (dB) φ=90º**	**HPBW(º) φ=90º**
RO3003	1.6 (6.8 %)	-18	18	-22	22
PP	1.4 (5.8%)	-17	15	-20	16

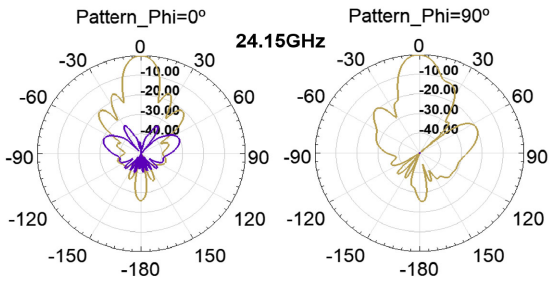

Fig. 3. Radiation pattern results at 24.15 GHz: cuts for Phi=0º and Phi=90º. The khaki traces are for copolarization (CP) and the violet ones for crosspolarization (XP)

IV. FABRICATION AND MEASUREMENT OF THE GAA

33µm and 80µm adhesive backed aluminum tapes are used respectively for the grid radiator and ground plane metallic parts of the GAA, in contrast to a 35µm tin-copper tape used in a recent work [14]. The aluminum is recyclable and eco-friendly, lighter and more flexible than copper. Only a limited number of widths of adhesive aluminum tape are available on the market. A wider one, but also thicker, was required for the ground plane, whereas a narrower one and also thinner was used for the radiator. In contrast to simple geometry patch type array, quite easy to fabricate with laser micromachining [14], PP GAA comprises many slots (one for each loop) into which adhesive residue is stuck when the laser heats the aluminum before removal (without a prior intensive and rather time-consuming ad-hoc improvement of the fabrication files) which leads to potential impairments. Thus, conventional milling machining with LPKF protomat machine was used to fabricate the antenna prototypes on Cu-cladded RO3003 and aluminium-cladded PP. SMA connector operating up to 26GHz was respectively soldered on RO3003 GAA and fixed with silver-epoxy adhesive on PP GAA by hand.

A. *Impedance matching of the GAA prototypes*

Both prototypes of GAA antenna on RO3003 and PP exhibit proper impedance matching in the target 24.05GHz-24.25GHz band. However, simulations do not account for the connectorization effects (soldering in RO3003 and fixing in PP) and manufacturing tolerances (especially for the PP).

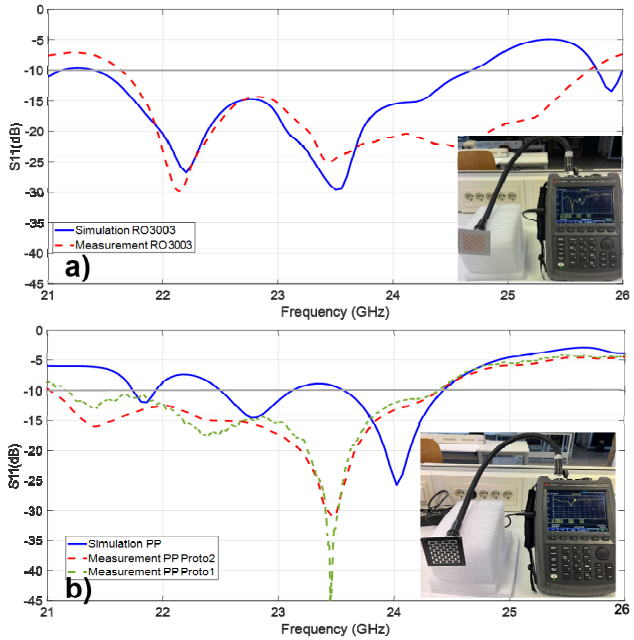

Fig. 4. Measurement results of the reflection coefficient, S_{11} (dB), for the fabricated array antenna on RO3003 (a) and aluminum plated PP (b) versus the simulation results.

B. *Radiation Characteristics of the GAA prototypes*

The GAA prototypes on both RO3003 and PP were measured in an anechoic chamber using a 3D printed polylactic Acid (PLA) based piece (see Fig. 5) for fixing the antenna to that aim.

As expected, pencil-beam patterns are obtained for both Phi=0° and Phi=90°, with HPBW and SLL almost identical to simulations (see Fig. 6). XP levels have raided but are still good for the target application. The good repeatability of the manufacturing technology can be verified since 2 prototypes on PP exhibit similar S_{11} and G (see Fig. 4 and TABLE IV.). The peak gain was measured with intercomparison of the GAA with a Flann Microwave Standard Horn 20240-25. The measured GAA on RO3003 agrees better with simulation in terms of G (1.1dB mismatch). The S_{11} of the GAA on PP is shifted-down in frequency, and so does the band for agreement in terms of G (see PP Proto 2 in TABLE IV.). In addition to the cable and connector fixing (not included in simulation), reflections in the set-up and misalignment with the horn can disturb the G results [17].

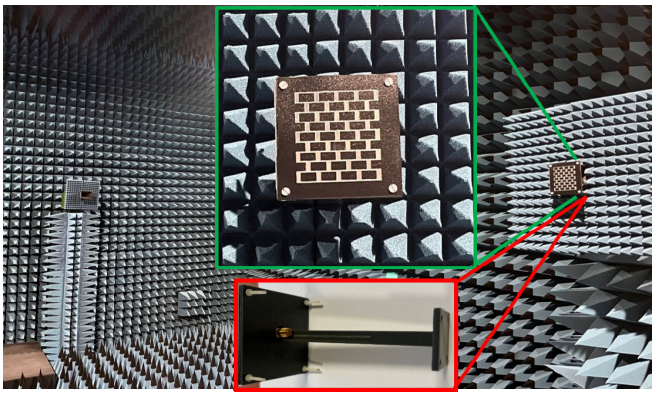

Fig. 5. Measurement set-up in anechoic chamber. Antenna under test (AUT) arrangement and prototype of GAA on PP.

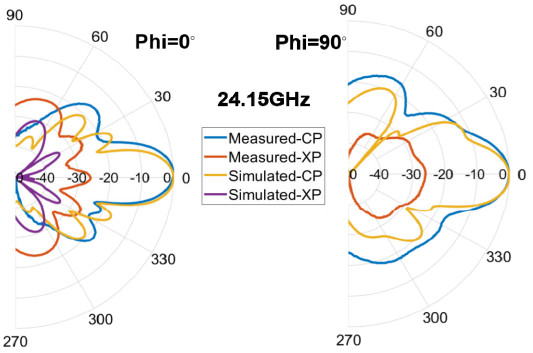

Fig. 6. Simulated vs measured co-polar (CP) and cross-polar (XP) components of the GAA on PP for Phi=0º and Phi=90º cuts at 24.15 GHz.

TABLE IV. RADIATION PROPERTIES RESULTS IN MEASUREMENTS

Freq (GHz)	G (dBi)		
	RO3003	PP proto1	PP proto2
24.05	16.9	16.2	15.8
24.15	16.6	15.7	15
24.25	16.5	15.3	14.8
23.45	–	–	18.8
23.55	–	–	18.6
23.65	–	–	18.24

The discrepancies between the simulated and measured $|S11|$, Gain, pattern deformation and cross-polarization level rise, were mainly caused by manufacturing tolerances, and connectorization. It is worth carrying out a deep analysis of the factors with the most critical impact, so as to improve manufacturing and to propose strategies aiming at a potential introduction in the market of aluminium-cladded PP.

Inaccuracies in the PP electromagnetic characterization are ruled out, since very good agreement in S_{11} was obtained in [14] with such ε_r and tanδ, and a parametric swept on them does not explain the variations in the radiation pattern cuts. However, manufacturing tolerances are critical, especially as regards W_l and W and, to a lesser extent, L and W_s. The shift down in frequency and gain reduction are attributable to under-etching W_l (0.1mm yields 1.6dB gain reduction) and over-etching W (0.25 mm yields 3.5dB gain reduction). The later also accounts for the XP level increase and CP deformation for both Phi=0° and Phi=90°. Under-etching L (0.1mm yields 0.5dB gain reduction) and over-etching W_s (0.2 mm yields 0.2dB gain reduction) have less impact. In addition, the connector fixing was analysed by simulating a drop of silver loaded epoxy adhesive and hardener (ε_r=3.6 and tanδ=0.012 and ρ=1.75Ω/m). Increasing the drop diameter keeping it inside the strip, shifts-down the resonance and decreases G (0.32dB for a 0.4mm variation) and radiation efficiency. The same applies to the drop height. Variations on the silver loaded epoxy ε_r, tanδ and ρ were also considered, without achieving significant influence on G and XP level. Nonetheless, the curing of the conducing paste is also critical. Finally, it was found that the thick ground plane impacts the S_{11} and reduces 0.5dB the gain. Fig. 7 shows how the combination of the aforementioned factors explains the disagreement between simulation and measurements. The dimensions indicated on it provide G=17.6dBi at 24.15GHz (1.9dB mismatch, much closer to the RO3003 one).

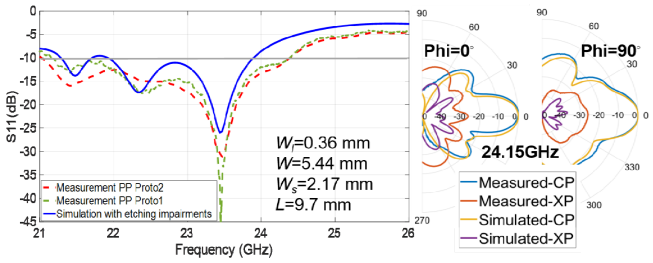

Fig. 7. Simulation vs measurements of S_{11} and radiation pattern cuts considering etching impairments and silver loaded epoxy drop

V. COMPARISON WITH OTHER ANTENNAS AT 24GHZ

Compared to antennas on substrates with ε_r values close to the one of PP (see TABLE V. and TABLE VI.), the presented GAA is thinner than [7] and more compact than

[14], and [18]-[20], while it exhibits wider bandwidth and higher or similar gain. The achieved SLL is very similar to the one of the other antennas. However, it overcomes [13]-[14] and [18]-[20] in terms of HPBW for Phi=90°, since GAA on PP exhibits pencil-beam pattern for both Phi=0° and Phi=90° cuts. Moreover, it provides the highest radiation efficiency among the considered antennas, which is critical for wearable applications and it is not generally provided.

TABLE V. SIZE, BANDWIDTH AND IMPEDANCE MATCHING

Ref.	Size (mm^3)	ε_r	Band (GHz)	BW (%)	S11 (dB)
[7]	60 x 60 x 0.787	2.2	1.99	8.2	-34
[13]	20 x 20x 0.68	2.9	2.0	8.3	-35
[14]	98.7x 14.4x0.52	2.2	0.28	1.2	-25
[18]	74.9x74.9 x 3.3	-	0.2	1.0	-8
[19]	160 x 43.2 x 0.5	2.3	0.32	1.3	-20
[20]	230 x 31x 0.254	2.17	0.39	1.6	-20
This work	60 x 60 x 0.52	2.2	0.96	4.0	-26

TABLE VI. RADIATION PROPERTIES

Ref.	G (dBi)	η (%)	SLL (dB) φ=0º	HPBW (º) φ=0º	SLL (dB) φ=90º	HPBW(º) φ=90º
[7]	20.6	-	-15	16	-25	16
[13]	7.4	35	-	54	-25	48
[14]	16.8	91	-18	9.2	-25	64
[18]	17	-	-20	12	-20	50
[19]	17	-	-18	8.2	-18	80
[20]	21.7	60	-21	3.6	-21	46
This work	20.8	98	-17	15	-20	16

VI. CONCLUSIONS

A low cost linearly polarized microstrip grid array antenna (GAA) was designed and fabricated on eco-friendly aluminum-cladded PP, exhibiting suitable properties for 24GHz wearable applications, such as collision avoidance radar in aid of visually impaired people, given its compact outline dimensions, its lightness and flexibility, the reduced FTBR and high radiation efficiency. Moreover, it contributes to circular economy due to the recyclability of both dielectric and metallic materials, while it reduces the environmental footprint of electronics.

This work has open up several questions that require further investigation concerning improvements on the fabrication and the sensitivity to connector fixing.

ACKNOWLEDGMENT

This research was funded by Ministerio de Ciencia, Innovación y universidades of Spanish Government under project META-IMAGER PID2021-122697OB-I00 and by Gobierno del Principado de Asturias under project IDI/2021/000097

REFERENCES

[1] J. Shan, K.Rambabu, Y.Zhang, J. Lin, "High gain array antenna for 24 GHz FMCW automotive radars", AEU - International Journal of Electronics and Communications, Vol. 147, 2022, 154144.

[2] J. Kraus, "A backward angle-fire array antenna," in IEEE Transactions on Antennas and Propagation, vol. 12, no. 1, pp. 48-50, January 1964, doi: 10.1109/TAP.1964.1138171.

[3] R. Conti, J. Toth, T. Dowling and J. Weiss, "The wire grid microstrip antenna," in IEEE Transactions on Antennas and Propagation, vol. 29, no.1, pp.157-166,January 1981, doi: 10.1109/TAP.1981.1142541.

[4] H. Nakano, T. Kawano, J. Yamauchi, 'Meander-line grid-array antenna', IEE Proc. Microw. Antennas Propag., 1998, 145, (4), pp. 309– 312. doi: 10.1049/ip-map:19981879.

[5] H. Nakano, Y. Iitsuka and J. Yamauchi, "Rhombic Grid Array Antenna," in IEEE Transactions on Antennas and Propagation, vol. 61, no. 5, pp. 2482-2489, May 2013.

[6] L. Zhang, W. Zhang and Y. P. Zhang, "Microstrip Grid and Comb Array Antennas," in IEEE Transactions on Antennas and Propagation, vol. 59, no. 11, pp. 4077-4084, Nov. 2011, doi: 10.1109/TAP.2011.2164216.

[7] Z. Chen and Z. Y. Ping, "24-GHz microstrip grid array antenna for automotive radars application," 2015 IEEE 5th Asia-Pacific Conference on Synthetic Aperture Radar (APSAR), 2015, pp. 125-127, doi: 10.1109/APSAR.2015.7306170.

[8] S. Assimonis, T. Samaras, V. Fusco, "Analysis of The Microstrip-Grid Array Antenna and Proposal of A New High-Gain, Low-Complexity, and Planar Long-Range WiFi Antenna". IET Microwaves, Antennas and Propagation, 12(3), 332-338. 2017.

[9] M. E. de Cos Gómez, H. Fernández Álvarez, A. Flórez Berdasco, and F. Las-Heras Andrés, "Paving the Way to Eco-Friendly IoT Antennas: Tencel-Based Ultra-Thin Compact Monopole and Its Applications to ZigBee," Sensors, vol. 20, no. 13, p. 3658, Jun. 2020.

[10] M. E. de Cos and F. Las-Heras, "Polypropylene-Based Dual-Band CPW-Fed Monopole Antenna [Antenna Appcations Corner]," in IEEE Antennas and Prop. Mag., vol.55, no.3, pp. 264-273, June 2013

[11] L. Garcia-Gamez, L. Bernard, S. Collardey, H. Covic, R. Sauleau, K. Mahdjoubi, P. Potier and P. Pouliguen, "Compact GNSS Metasurface-Inspired Cavity Antennas," in IEEE Antennas and Wireless Propagation Letters, vol. 18, no. 12, pp. 2652-2656, Dec. 2019, doi: 10.1109/LAWP.2019.2947791

[12] A. Causse, K. Rodriguez, L. Bernard, A. Sharaiha, and S. Collardey, "Compact Bandwidth Enhanced Cavity-Backed Magneto-Electric Dipole Antenna with Outer Γ-Shaped Probe for GNSS Bands," Sensors, vol. 21, no. 11, p. 3599, May 2021, doi: 10.3390/s21113599

[13] M Poggiani, P Mezzanotte, C Mariotti, M Virili, G Orecchini, F Alimenti, et al., "24 GHz patch antenna network in cellulose-based materials for green wireless internet applications", Science measurement and Technology IET, vol. 8, no. 6, pp. 342-349

[14] M. E. de Cos Gómez, H. F. Álvarez and F. L. -H. Andrés, "Millimeter Wave Antenna on Eco-friendly Substrate for Radar Applications," 2022 16th European Conference on Antennas and Propagation (EuCAP), 2022, pp. 1-5, doi: 10.23919/EuCAP53622.2022.9769364.

[15] Rogers Corp Laminates. Datasheet of RO3003. Available online: https://rogerscorp.com/advanced-electronics-solutions/ro3000-series-laminates/ro3003-laminates (Accessed on 18 Sep 2022)

[16] K. . -P. Latti, M. Kettunen, J. -P. Strom and P. Silventoinen, "A Review of Microstrip T-Resonator Method in Determining the Dielectric Properties of Printed Circuit Board Materials," in IEEE Transactions on Instrumentation and Measurement, vol. 56, no. 5, pp. 1845-1850, Oct. 2007, doi: 10.1109/TIM.2007.903587

[17] "IEEE Recommended Practice for Antenna Measurements," in IEEE Std 149-2021 (Revision of IEEE Std 149-1977) , vol., no., pp.1-207, 18 Feb. 2022, doi: 10.1109/IEEESTD.2022.9714428.

[18] SAM-2432431750-KF-L1 K Band Microstrip Patch Array Antenna https://sftp.eravant.com/content/datasheets/SAM-2432431750-KF-L1.pdf

[19] Y. Jung, D. Park and C. W. Jung, "Low cost 24GHz patch array antenna for high sensitivity EM sensor," 2010 Asia-Pacific Microwave Conference, 2010, pp. 2208-2211.

[20] M. Slovic, B. Jokanovic and B. Kolundzija, "High efficiency patch antenna for 24 GHz anticollision radar," TELSIKS 2005 - International Conference on Telecommunication in ModernSatellite, Cable and Broadcasting Services, 2005, pp. 20-23 vol. 1